Catalysis Letters Vol. 101, Nos. 3–4, June 2005 (© 2005)
DOI: 10.1007/s10562-004-4895-6

Reproducibility of highly active Au/TiO_2 catalyst preparation and conditioning

B. Schumacher[a,*], V. Plzak[b], J. Cai[a], and R.J. Behm[a]

[a]*Department Surface Chemistry and Catalysis, University of Ulm, D-89069 Ulm, Germany*
[b]*Centre for Solar Energy and Hydrogen Research, Helmholtzstr. 8, D-89081 Ulm, Germany*

Received 23 June 2004; accepted 03 July 2004

We present results of a comparative study on the reproducibility of Au/TiO_2 catalyst preparation and conditioning. Comparison of their physical characteristics and their catalytic activity for CO oxidation shows that highly active catalysts can indeed be prepared in a very well-defined and reproducible way, with particle sizes of ~2 nm (conditioning *via* reductive or redox treatment) or ~3 nm (conditioning *via* calcination).

KEY WORDS: Au/TiO_2 catalyst; reproducibility; CO oxidation; selective particle size; TEM; oxidation state; XPS.

1. Introduction

Highly disperse, metal oxide supported Au catalysts have been found to be extremely active for various oxidation and hydrogenation reactions, in particular for CO oxidation, already at low temperatures [1–4]. For instance, Au/TiO_2 catalysts were reported to be active for CO oxidation even at 90 K [5]. Commonly, highly active Au/TiO_2 catalysts are prepared *via* deposition–precipitation (DP) or *via* coprecipitation (CP) and subsequently calcined in air at temperatures between 200 °C and 400 °C [6–12]. A common problem with these Au catalysts, however, is the insufficient reproducibility in their preparation and conditioning [1–4,13]. In order to elucidate this question in more detail we performed a comparative study on a series of four Au/TiO_2 catalysts with similar Au loadings and one more catalyst with a higher loading, which had been prepared separately, but along the same DP procedure, which had been described earlier [11]. The higher loading catalyst was included in order to evaluate a possible influence of the Au loading on the activity. In order to include possible effects of the conditioning procedure all of these catalysts were conditioned following three different, typical conditioning procedures: (i) calcination at 400 °C, (ii) reduction at 200 °C and (iii) a redox conditioning procedure including reduction at 200 °C and subsequent oxidation at 300 °C.

The catalysts were compared with respect to their physical characteristics such as particle size, particle size distribution and surface composition, which were determined by transmission electron microscopy (TEM) and X-ray photoelectron microscopy (XPS), and their catalytic activity and stability for CO oxidation, both in a H_2-free and in a H_2-rich atmosphere. Measurements in a H_2-free atmosphere were performed with catalysts conditioned *via* calcination and *via* redox treatment, respectively, measurements in H_2-rich atmosphere included catalysts conditioned *via* calcination and *via* reductive treatment, respectively. The measurements in H_2-rich atmosphere were carried out due to the fact that this catalyst system could be attractive for the clean-up of reformer gas from CO impurities in feed streams for polymer membrane (PEM) fuel cells [14]. Therefore, the selectivity for CO oxidation was determined as an addition catalytic property in these measurements. For the same reason the reaction temperature we chose a reaction temperature of 80 °C.

* To whom correspondence should be addressed.
E-mail: birgit.schumacher@chemie.uni-ulm.de

2. Experimental

2.1. Preparation of the Au/TiO_2 catalysts

TiO_2 powder (Degussa P25) was suspended in water at 60 °C. Then an aqueous solution of $HAuCl_4 \cdot 4H_2O$ was added at constant temperature while the suspension was stirred. The pH of the solution was kept constant at about 5–5.5 by adding a 0.16 M solution of Na_3CO_2. Subsequently stirring was continued for additional 30 min. The precipitates were cooled, filtered and washed. Afterwards the filtrates were dried over night at room temperature in vacuum. The Au metal contents were determined *via* inductively coupled plasma atom emission spectroscopy (ICP-AES). Five different samples, denoted as Au/TiO_2(A) (3.4 wt% Au), Au/TiO_2(B) (3.4 wt% Au), Au/TiO_2(C) (3.0 wt% Au), Au/TiO_2(D) (5.4 wt% Au), and Au/TiO_2(E) (3.4 wt% Au), were prepared. The BET surface of all catalysts was 56 m^2.

Three different, often applied conditioning procedures were used: (i) conventional conditioning by calcination in 10% O_2/N_2 at 400 °C for 30 min [1,6–12], (ii) a reductive conditioning procedure including 45 min annealing in 10% H_2 in N_2 at 200 °C, which was described also in a previous paper [11] and (iii) a redox conditioning procedure including 45 min annealing in 10% H_2 in N_2 at 200 °C and subsequent 30 min calcination in 10% O_2 in N_2 at 300 °C. Examples for the latter type of conditioning procedure can be found in refs. [15–17], though the exact processing temperatures were different. After conditioning the samples were cooled down in N_2 to the reaction temperature of 80 °C.

2.2. Catalyst characterization

The gold particle sizes were determined for all five catalysts after each of the three different conditioning procedures by transmission electron microscopy (TEM), using a Philips CM 20 microscope (200 kV). For each sample at least 300 particles were evaluated.

The relative concentrations and the oxidation states of Au, Ti and O surface atoms were determined by X-ray photoelectron spectroscopy (XPS) (PHI 5800 ESCA system) using monochromatised Al-K_α radiation. Spectra were recorded from all five catalysts in the unconditioned state and after the three conditioning procedures. Background subtraction and peak fitting was performed using a public XPS peak fit program (XPSPEAK4.1 by R. Kwok). In order to exclude surface charging effects the binding energies (BEs) were calibrated using the Ti $2p_{3/2}$ peak as reference. Its binding energy (BE) was set to 459.2 eV, the reported value for anatase and rutile [18]. For all samples the Ti $2p_{3/2}$ could be well described by a single component related to Ti^{4+} species, contributions from lower oxidation states can not be resolved. For comparison of the catalysts the peak areas were normalized to the peak area of Ti 2p signal in the redox conditioned sample of catalyst Au/TiO_2(D). Fits of the Au 4f peaks were performed based on the following assumptions: (i) the difference between Au $4f_{7/2}$ and $4f_{5/2}$ was set to 3.67 eV, (ii) the integral intensity of the Au $4f_{5/2}$ peak is three quarters of that of the Au $4f_{7/2}$ peak, and (iii) the peak widths (FWHM) for both peaks are equal. Furthermore the Lorenz-Gauss ratio for each Au species was kept constant. For the fits of the O 1s peak the FWHMs were kept constant. For both TEM and XPS measurements catalyst conditioning was performed *ex situ*.

2.3. Activity measurements

Activity measurements were performed at atmospheric pressure in a quartz tube micro reactor (i.d. 4 mm) located in a ceramic tube oven, with typically 100 mg catalyst powder (catalyst bed length 5–8 mm). The catalyst samples were diluted with α-Al_2O_3, which is not active for CO oxidation under present conditions, in order to obtain differential reaction conditions. The reactions were carried out with a flux of 60 NmL/min (space velocity 41,000 h^{-1}) at 80 °C in two different atmospheres: (i) in a H_2-rich atmosphere containing 1 kPa CO, 1 kPa O_2, 75 kPa H_2, balance N_2 and (ii) in a H_2-free atmosphere containing 1 kPa CO, 1 kPa O_2, balance N_2. The influent and effluent gas was analyzed by on-line gas chromatography (Dani GC 86.10HT). High purity reaction gases (CO 4.7, O_2 5.0, H_2 5.0, N_2 6.0 from Westphalen) were used. Evaluation of the Weisz criterion showed the absence of mass-transport-related problems [19]. For further details, in particular on the determination of activities and selectivities, see [20].

3. Results and discussion

3.1. Physical characterization before and after conditioning

3.1.1. Au particle sizes

TEM images of the five catalysts show well separated Au particles (dark spots) on the larger TiO_2 substrate particles for each of the three conditioning procedures, which is demonstrated in the TEM images of Au/TiO_2(A) (50 nm × 50 nm) in figure 1. Obviously, the Au particles in the calcined sample (figure 1a) are bigger than those in the redox conditioned (figure 1b) and in the reductively conditioned samples (figure 1c), respectively. The particle size distributions of the Au/TiO_2(A) catalyst evaluated from the above and similar images, which are shown in figure 2, reproduce this trend: the calcined sample (figure 2a) exhibits a rather wide particle size distribution with a mean particle size of 3.0 nm ± 0.5 nm, the particles in the redox conditioned and the reductively conditioned samples have a much narrower particle size distribution with mean particle sizes of 2.0 nm ± 0.3 nm and 2.1 nm ± 0.4 nm, respectively. The particle size distributions of the other catalysts closely resemble these results, the mean particle sizes are listed in table 1. In all cases the calcination procedure leads to mean particle sizes of about 3 nm, whereas for the redox conditioned and for the reduced samples the particle sizes are around 2 nm. Interestingly, the increase in Au loading (sample (D)) does not lead to a measurable increase in particle size compared to the lower loading samples.

Previous studies of Au/TiO_2 catalysts prepared *via* deposition–precipitation procedures reported particle sizes ranging from 2.4 nm to 3.6 nm after 400 °C calcination [21], with [22–24] bigger particles resulting from longer calcination times. Likewise, Boccuzzi *et al.* reported a mean particle size of 2.4 ± 0.9 nm for a deposition–precipitation prepared catalysts after calcination at 200 °C [9], and Zanella *et al.* determined particle sizes of 2.3 ± 0.5 nm and 2.0 ± 0.4 nm, respectively, for a deposition–precipitation prepared

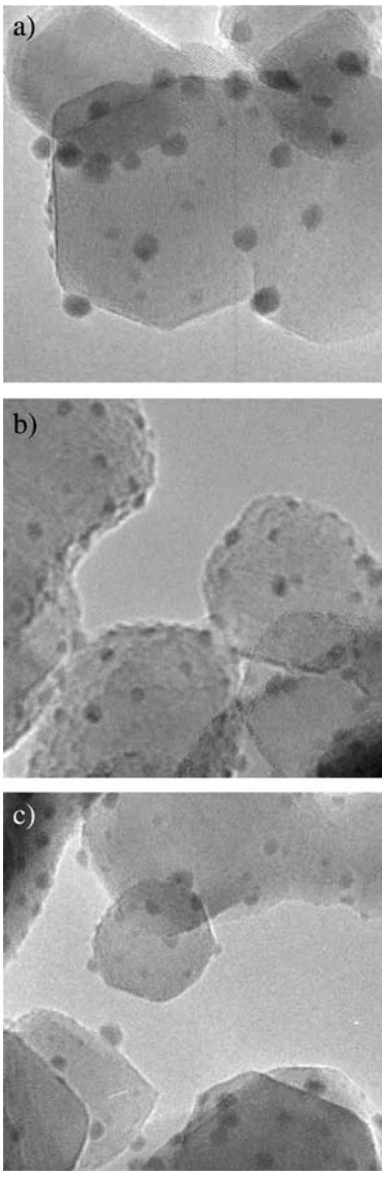

Figure 1. TEM images (50 nm × 50 nm) of catalyst Au/TiO_2(A) after (a) calcination, (b) redox conditioning and (c) reductive conditioning.

catalyst using urea and NaOH as pH controlling agent [23]. For a catalyst prepared *via* deposition–precipitation on an anatase support we previously obtained a particle size of 1.8 ± 0.5 nm after reductive treatment [11].

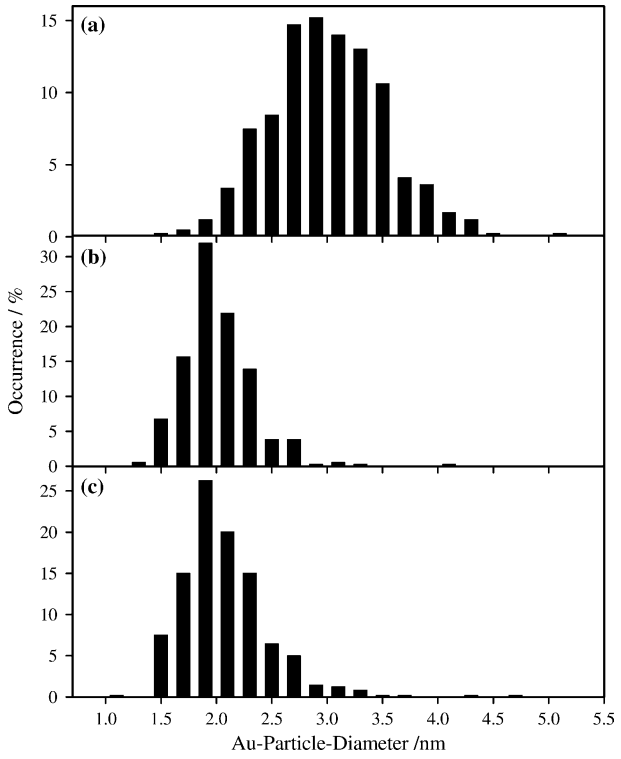

Figure 2. Particle size distribution of catalyst Au/TiO_2(A) after (a) calcination, (b) redox conditioning and (c) reductive conditioning.

Catalysts prepared via the incipient wetness method generally exhibit much larger Au particles than those prepared *via* deposition–precipitation [15,16,25]. For instance, a particle size of 30 nm, which is one order of magnitude larger than that of the present catalysts, was reported by Bollinger *et al*. for a catalyst prepared by the incipient wetness method (P25 support material) after reductive conditioning at 200 °C [15]. The smallest Au particles for this preparation method were reported by Ossipof *et al*. [25], who found a particle size of 7.3 nm after drying the catalyst at 120 °C. These values agree well with those determined in the present study. Apparently, the particle size is mainly controlled by the conditioning temperature, at least at the lower temperatures, while under these conditions the conditioning atmosphere is less important. It should be noted that recent results obtained for reactive annealing of planar

Table 1
Au particle sizes and dispersion after the three conditioning procedures

Sample	wt% Au	Calcination		Redox conditioning		Reduction	
		ø [nm]	Disp. [%]	ø [nm]	Disp. [%]	ø [nm]	Disp. [%]
A	3.37	3.0 ± 0.5	36.6	2.0 ± 0.3	54.7	2.1 ± 0.4	51.7
B	3.37	3.1 ± 0.5	35.7	1.9 ± 0.3	56.9	1.9 ± 0.4	58.3
C	2.96	3.1 ± 0.5	36.1	1.9 ± 0.4	52.7	1.7 ± 0.3	63.3
D	5.43	3.0 ± 0.5	36.5	2.0 ± 0.3	51.0	1.9 ± 0.3	57.7
E	3.37	3.3 ± 0.5	33.3	2.2 ± 0.4	49.9	1.9 ± 0.3	58.0

$Au/TiO_2(110)$ model catalysts in an O_2 atmosphere (50 mbar) and in air (1 atm.) showed significant changes in particle size for annealing temperatures of 300 °C and above, but not for room temperature exposure [26].

A redox conditioning procedure with an initial reduction step followed by a calcination step at a higher temperature has been developed in our laboratory based on activity tests in a reaction atmosphere, but related procedures, though at different temperatures, have also been reported from other groups [15,16,25,27,28]. For instance, Schimpf *et al*. reported that redox conditioning of a 1.7 wt% Au loaded catalyst (preparation *via* deposition–precipitation, support: Degussa P25), involving calcination at 300 °C for 8 h and reduction at 300 °C for 3 h, leads to Au particles with a mean diameter of 5.3 nm [27]. Since we did not find significant loading effects in this range, the much larger particle size of these catalysts, which is more than twice as high as the particle sizes of our redox conditioned samples, is attributed to the higher reduction temperature and the longer conditioning times.

3.1.2. Surface composition of the catalysts

The surface composition of the unconditioned catalysts and after the respective conditioning treatments was characterized by XPS, representative spectra recorded on the Au/TiO_2(A) catalyst are shown in figures 3 (Au 4f) and 4 (O 1s).

Au 4f. Figure 3 shows the Au 4f spectra of catalyst Au/TiO_2(A) in its unconditioned state (d) and after the three conditioning procedures (a–c). The peak of the unconditioned sample shows a significant shift to higher binding energies (BEs) compared to the conditioned samples, which can be explained by more oxidized species (initial state effect) and by final state effects due indicative of very small Au particles. The larger width of the Au 4f peak reflects a distribution of particle sizes. The peaks of the unconditioned samples were not fitted since they are expected to result from a whole series of peaks with continously increasing BE, due to the decreasing final state relaxation of the very small particles. The calcined samples consist only of metallic Au, with BEs between 83.9 eV and 84.0 eV (see table 2), which is in good agreement with literature values for bulk Au [4,8,29,30]. Fits of the Au 4f peaks of the redox conditioned and reductively conditioned samples show metallic Au as main component and small contributions of Au^{3+} species, which appear at 1.9 eV higher BE, at values of 85.7–86.0 eV, independent of conditioning procedure or gold loading. These values agree well with those reported by Holm and Storp [31] and Dickenson *et al*. [32].

In contrast to our findings Soares *et al*. found Au^{3+} contributions upon calcination up to temperatures of 450 °C for a catalyst prepared *via* the incipient wetness method, while a similar conditioning procedure resulted in purely metallic Au particles for deposition–precipitation prepared catalysts upon calcination at temperatures of 120 °C and higher [30].

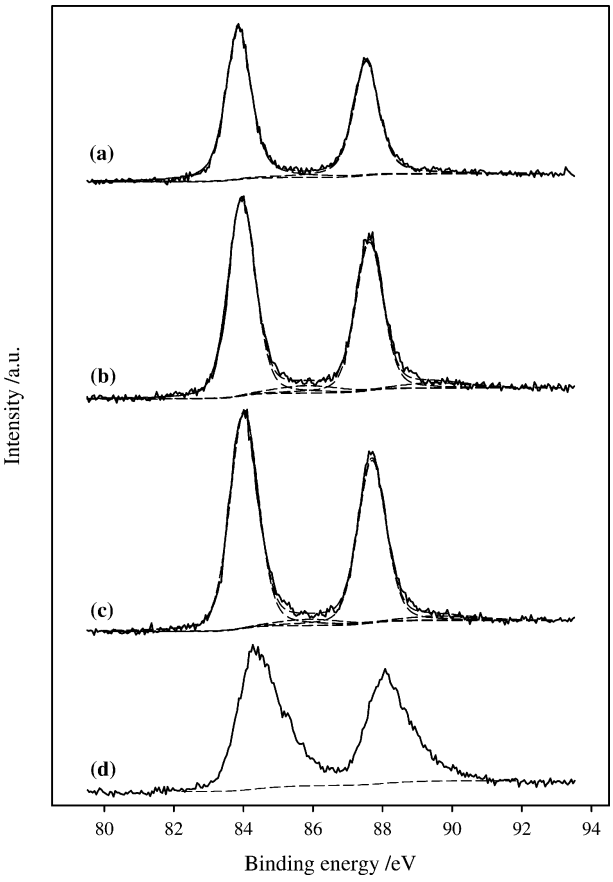

Figure 3. XPS Au 4f peaks of catalyst Au/TiO_2(A) after (a) calcination, (b) redox conditioning, (c) reductive conditioning and (d) of a unconditioned sample. Fits assume a FWHM of 0.9–1 eV and a $4f_{7/2}$:$4f_{5/2}$ intensity ratio of 4:3.

The binding energies of Au^0 and Au^{3+} signals, the Au/Ti intensity ratios (calculated from the peak areas with consideration of the sensitivity factors) and the Au^{3+}/Au^0 intensity ratios for all five catalysts are listed in table 2. The Au/Ti ratios are smaller after calcination than after the other two conditioning procedures, which agrees well with the bigger gold particles in these catalysts. Likewise, the small intensity differences between the redox conditioned and the reduced samples are consistent with the similar particle sizes determined after these conditioning procedures. The high reproducibility of the preparation is obvious when comparing the Au/Ti ratios of the different catalyst samples for each conditioning procedure. The variation between the samples with similar Au loading (catalysts Au/TiO_2(A), Au/TiO_2(B), Au/TiO_2(C), Au/TiO_2(E)), are very small. The Au^{3+}/Au^0 ratio (see table 2) is not as homogenous as the Au/Ti ratio. Here the variation between the values is 2–5-times as big as in the Au/Ti ratios. It should be noted that the higher loading catalyst Au/TiO_2(D), has a much smaller Au^{3+} relative intensity after redox conditioning than the other catalysts, indicating that Au

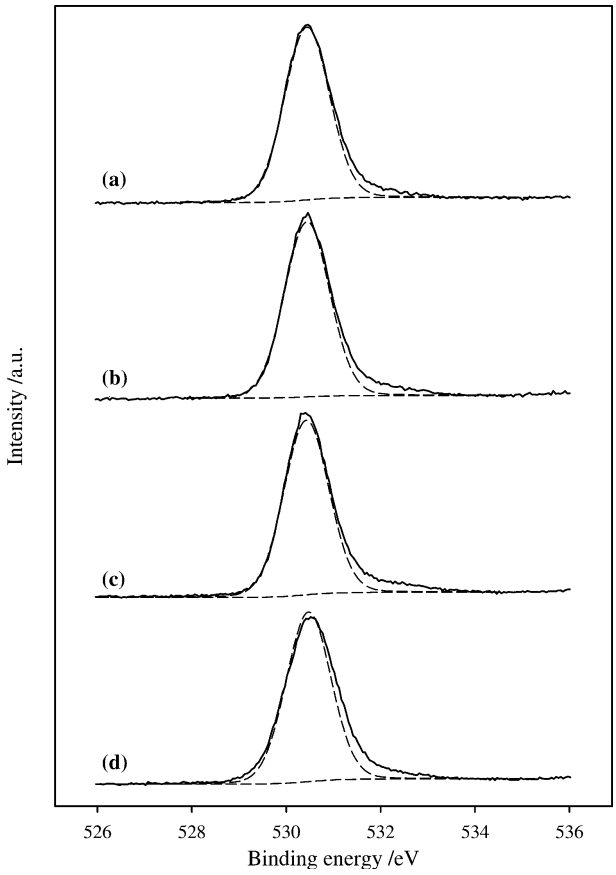

Figure 4. XPS O 1s peaks of Au/TiO_2(A) after (a) calcination, (b) redox conditioning, (c) reductive conditioning and (d) of un unconditioned sample.

reduction is not adversely affected by the higher Au content. After reductive conditioning the trend is similar, but the effect is not as pronounced. In contrast to the other catalysts, sample Au/TiO_2(D) does not show a higher amount of Au^{3+} after redox conditioning than after reduction, i.e., reoxidation in the second conditioning step is less efficient than for the other catalysts.

O 1s. XPS spectra of the O 1s peak of catalyst Au/TiO_2(A) in its unconditioned state and after the three conditioning procedures are shown in figure 4. Clearly, neither the position nor the intensity of the peak show any significant effect of the conditioning procedures. For all samples the main O 1s peak resulting from TiO_2 can be fitted by a peak with constant width (FWHM 1.1 eV) and a constant Lorenz-Gauss ratio. The BEs for this O 1s species, which are between 530.4 and 530.5 eV and the resulting O/Ti ratios for all catalysts in their unconditioned and conditioned states are listed in table 3. The BE agrees well with data on TiO_2 (rutile) from Dupin *et al*. [33], who found a main O 1s peak at 530.0 eV and a shoulder at 531.8 eV, where the latter contributes about 13% to the total intensity. Considering that they reported a BE of 458.7 eV for the corresponding Ti $2p_{3/2}$ peak, which is 0.5 eV lower than the reference value used here, their data fit excellently to the results reported here. These authors assigned the high BE shoulder at 531.8 eV (corrected 532,3 eV) to either weakly adsorbed species or to subsurface oxygen that could be described as O^- species [33]. The spectra in figure 4 also show a shoulder at similar, higher BEs. While we cannot exclude the above assignment of subsurface oxygen, we favor to explain this by contributions from surface hydroxyl and carbonate species, which, based on diffuse reflectance IR spectroscopy (DRIFTS) data from our laboratory (spectra not shown here), are present under these conditions. The existence of OH-groups on the support could be observed even after conditioning at 400 °C; a similar behaviour was reported also by Martra [34] and carbonate species begin to form on this catalyst as soon as it is exposed to a CO_2 containing atmosphere, e.g., during transport through air. Finally, this shoulder also contains contributions from the Au_2O_3 detected in the Au 4f spectra of the redox conditioned and reduced samples. Their intensity, however, is negligible, and would be far from sufficient to explain the high BE shoulder.

Besides the binding energies of the main O 1s signal from TiO_2, table 3 also shows the O/Ti concentration ratios of the main O 1s signal related to O^{2-} from TiO_2 and of the complete peak. The O_{TiO2}/Ti concentration ratios are close to 2, as expected from the stoichiometry of TiO_2. On the other hand, since about 10–15% of the intensity of the O 1s peak result from OH groups and carbonate like species, the O_{Ges}/Ti concentration ratios are significantly higher, between 2.2 and 2.3 (see in table 3).

Table 2
Binding energies and relative intensities of the Au $4f_{7/2}$ signal after the three conditioning procedures

Sample	Calcination		Redox conditioning				Reductive conditioning			
	BE(Au^0) [eV]	I(Au)/ I(Ti)	BE(Au^0) [eV]	BE(Au^{3+}) [eV]	I(Au^{3+})/ I(Au^0)	I(Au)/ I(Ti)	BE(Au^0) [eV]	BE(Au^{3+}) [eV]	I(Au^{3+})/ I(Au^0)	I(Au)/ I(Ti)
A	83.9	0.043	84.0	85.9	0.078	0.059	84.0	85.9	0.058	0.066
B	83.9	0.043	83.8	85.7	0.069	0.060	84.0	85.9	0.063	0.064
C	83.9	0.038	83.9	85.8	0.074	0.053	84.0	85.9	0.050	0.054
D	84.0	0.083	84.1	86.0	0.051	0.094	83.9	85.8	0.052	0.103
E	83.9	0.042	83.9	85.8	0.088	0.061	84.1	86.0	0.075	0.066

Table 3
Binding energies and relative intensities of the O 1s signal of the unconditioned catalyst and of the conditioned catalysts after the respective treatments

Sample	Untreated			Calcination			Redox conditioning			Reductive conditioning		
	BE [eV] $O–TiO_2$	$I(O_{TiO2})/I(Ti)$	$I(O_{tot})/I(Ti)$	BE [eV] $O–TiO_2$	$I(O_{TiO2})/I(Ti)$	$I(O_{tot})/I(Ti)$	BE [eV] $O–TiO_2$	$I(O_{TiO2})/I(Ti)$	$I(O_{tot})/I(Ti)$	BE [eV] $O–TiO_2$	$I(O_{TiO2})/I(Ti)$	$I(O_{tot})/I(Ti)$
A	530.5	1.93	2.17	530.4	1.96	2.13	530.4	1.99	2.21	530.4	2.01	2.32
B	530.4	1.79	2.30	530.5	2.01	2.20	530.5	1.98	2.70	530.5	2.05	2.24
C	530.4	2.00	2.28	530.5	1.97	2.14	530.4	2.01	2.25	530.5	2.04	2.35
D	530.4	1.94	2.38	530.4	2.00	2.23	530.4	2.04	2.23	530.5	2.00	2.28
E	530.4	1.99	2.25	530.4	1.98	2.19	530.4	1.96	2.23	530.4	2.05	2.23

3.2. *Activity, long term stability and selectivity of the $AuTiO_2$ catalysts*

3.2.1. *Catalytic activity after calcination*

The evolution of the CO oxidation reaction rates on the calcined catalysts is shown in figure 5a, both for reaction in H_2-free atmosphere (empty symbols) and in H_2-rich atmosphere (filled symbols). Clearly, deactivation in H_2-free atmosphere is much more pronounced than in H_2-rich atmosphere. After 1000 min on stream the activity in H_2-rich atmosphere has decayed to 70–80% of the initial value, in H_2-free atmosphere it decreased even to 15–35% for samples A, B, C and E and 10% for the high loading catalyst D. Both the initial activities as well as the deactivation behaviour of the four catalysts Au/TiO_2(A), Au/TiO_2(B), Au/TiO_2(C), Au/TiO_2(E) is very similar in both reaction atmospheres, only the high loading catalyst Au/TiO_2(D) shows a lower activity than the other samples. Diffuse reflectance IR measurements of catalyst Au/TiO_2(B) in the two atmospheres (spectra not shown here) indicate that in H_2-free atmosphere significant amounts of carbonates are generated during reaction, whereas in H_2-rich atmosphere carbonate formation is much less active, instead adsorbed H_2O is observed. This behaviour agrees well with our recent findings for a Au/TiO_2 catalyst supported on anatase [11,12], except for the much stronger deactivation of the present, anatase/rutile supported catalyst in a H_2-free atmosphere compared to the anatase supported catalyst. Apparently, the addition of rutile enhances the tendency for deactivation during CO-oxidation.

Comparing our results with the deactivation behavior in previous studies we find, despite of rather good agreement with several reports, no unique trend. Zanella *et al.* found a significant deactivation during CO oxidation at 5 °C in 1% CO, 2% O_2 , balance N_2 for catalysts which were equally prepared *via* deposition–precipitation using Degussa P25 as support material, if these catalysts were calcined at temperatures ≥200 °C [23]. After 5 h on stream the activities decreased to ~20–75% of the initial values. The deactivation behaviour and the reaction rates depended strongly on the calcination temperature: the higher the calcination temperature, the lower the reaction rates and the stronger the deactivation. For catalysts prepared using NaOH for pH control and subsequent calcination at low temperatures (100–150 °C) these authors found a small, initial activation of the catalyst, followed by a slow deactivation. Park *et al.* reported a slight deactivation during 5 h on stream in 1% CO, 5% O_2, balance N_2 at a

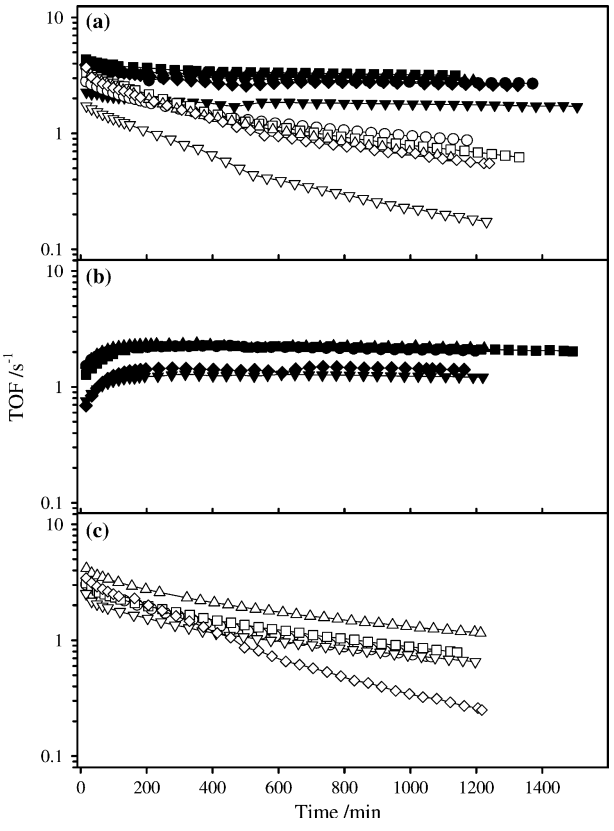

Figure 5. Long-term stability and deactivation of catalysts during reaction in different atmospheres. (a) Activity of the calcined catalysts in H_2-rich (1 kPa CO, 1 kPa O_2, 75 kPa H_2, balance N_2, filled symbols) and H_2-free atmosphere (1 kPa CO, 1 kPa O_2, balance N_2, empty symbol). (b) Activity of the reductively conditioned catalysts in H_2-rich atmosphere (1 kPa CO, 1 kPa O_2, 75 kPa H_2, balance N_2), and (c) of the redox conditioned catalysts in H_2-free atmosphere (1 kPa CO, 1 kPa O_2, balance N_2). ○: Au/TiO_2(A), □: Au/TiO_2(B), △: Au/TiO_2(C), ∇: Au/TiO_2(D), ◇: Au/TiO_2(E).

reaction temperature of 50 °C for catalysts. prepared *via* deposition–precipitation and calcined at different temperatures for 5 h [35]. Similar to the findings of Zanella *et al*. the reaction rates were higher after lower calcination temperatures. Konova *et al*. found a deactivation of about 50% of the initial activity during 1000 min CO-oxidation at room temperature in 0.06–0.24 vol% CO in air for catalysts prepared *via* deposition–precipitation and subsequent calcination in air at 120 °C for 1 h [36]. On the other hand, *Arri et al*. did not observe any deactivation of a Au/TiO_2 catalysts prepared *via* laser vaporization, upon CO-oxidation at 160 °C in 2% CO, 2% O_2, balance He during 70 h on stream [37]. Equally, Mallick *et al*. did not see any deactivation during 200 min in 10% CO, 10% O_2, balance He at different reaction temperatures for a catalyst prepared via deposition–precipitation on Degussa P25 [38]. It should be noted, however, that in the two latter studies very high amounts of catalyst were used, resulting in conversions of ≥ 80%, and it can not be excluded that the observed stability is an artifact caused by the presence of 'unused' catalyst.

The (initial) reaction rates in figure 5a are comparable with those of 'good' catalysts reported in literature. Extrapolating the published TOF numbers to a reaction temperature of 80 °C with the given activation energies, one obtains values in the range of 1.0 s^{-1} to 3.5 s^{-1} (note that the small differences in partial pressures where not corrected) [1,16,39,40]. For a model catalysts even a TOF of 4 s^{-1} at 80 °C was published [41].

Finally, the decreasing (mass normalized) activity of the Au/TiO_2 with higher Au content (catalyst (D)) in both atmospheres compared to that of the other samples can be compared with findings by Zanella *et al*. [23], who observed about similar TOF based activities for a 3.1 wt% Au containing catalyst (prepared *via* deposition–precipitation, pH control with NaOH) and a 7.6 wt% Au containing catalyst (prepared by deposition–precipitation, pH control with urea), 0.095 s^{-1} and 0.08 s^{-1}, respectively, interpolating to a similar particle size of 3 nm for both catalysts. It should be noted that in the above examples not only the Au content, but also the preparation procedure was changed slightly, while in our case only the Au content is varied. Since despite of the higher loading in sample (D) the mean Au particle size is similar to that of the other samples, and also the BET surface areas are similar, the main difference between the higher and lower loading catalysts in our series is the average support area surrounding each Au particle. We therefore speculate that the size of the substrate zone around each Au particle plays an important role for the activity of the catalyst.

3.2.2. *Catalytic activity after reductive and redox treatment*

The reaction rates for CO-oxidation on the reductively pretreated catalyst in H_2-rich atmosphere and of the redox-conditioned catalyst in H_2-free atmosphere are shown in figure 5b and c, respectively. The choice of the conditioning procedures for the two different reaction atmosphere was based on preceding tests, which had shown that the activity of a reductively conditioned catalyst in H_2-free atmosphere could be improved by a subsequent calcination step at temperatures low enough to avoid additional particle growth. For reaction in H_2-rich atmosphere, subsequent calcination did not improve the activity. Similar to the calcined catalyst we find a pronounced deactivation for the redox conditioned catalyst in H_2-free atmosphere. Within 1000 min reaction time the activity of catalysts Au/TiO_2(A), Au/TiO_2(B), Au/TiO_2(C) and Au/TiO_2(D) decreased to 25–35% of the initial values, that of catalyst Au/TiO_2(E) to 10%. I.e., while the initial activities are comparable to those of the calcined catalysts, in this case the reproducibility is significantly worse than after calcination, the tendency for deactivation (not the initial activity) of sample (E) deviates considerably from that of the other samples. Also the loading effect is not as pronounced as for the calcined catalysts, the activity of the high loading sample (D) is only little less than that of the other lower loading catalysts. While we have no satifactory explanation in the moment for the strong deactivation of catalyst (E), it should be noted that this catalyst has the highest relative Au^{3+} amount after redox-conditioning (see table 2).

Redox conditioning was also applied by other groups, but examples are much more scarce than for calcination [15–17]. In general, the reduction step was carried out at a higher temperature than the (subsequent) calcination step. Choudhary *et al*. found only little deactivation during CO oxidation at high O_2-excess of ($p_{O2} = 2 \cdot p_{CO} = 36.7$ mbar, reaction temperatures 40 °C and 80 °C) for a catalyst prepared *via* deposition–precipitation of a Au–phosphine complex on Degussa P25 and subsequent conditioning *via* reduction at 500 °C followed by calcination at 400 °C [17]. The conversion in their experiments was at least 50%, and the deactivation could even be decreased by redox regeneration cycles. Bollinger and Vannice, who studied the deactivation of a catalyst prepared *via* coprecipitation and subsequent conditioning *via* first reduction at 500 °C in H_2 for 1 h, followed by a calcination step at 400 °C for 1 h and finally low temperature reduction at 200 °C for 2 h, reported a deactivation to 60% and 26% of the initial activity during CO oxidation within 3 h in a H_2-free atmosphere with $p_{O2} = p_{CO} = 50$ mbar at reaction temperatures of 27 °C and 0 °C (differential conversions, particle size 4.5 nm, initial activity (TOFs) 0.076 s^{-1} at 27 °C and 0.053 s^{-1} at 0 °C), respectively [16]. Lin *et al*. who applied the same conditioning procedure for a catalyst prepared by the incipient wetness method, reported a deactivation to ~45% of the initial activity upon 1000 min CO oxidation at 40 °C ($p_{O2} = p_{CO} = 50$ mbar and $p_{CO} = 2 \cdot p_{O2} = 9.3$ mbar,

particle size ~30 nm, initial activity (TOF) at 87 °C 0.24 s^{-1}) [15]. The deactivation behaviour in [16] at 27 °C is in the range of the results presented here, the catalysts in [17] and [15] show a better stability. However, the reaction rates in [16] and [15] (in [17] no reaction rates were reported) are lower than those presented here after redox conditioning, even after a stronger deactivation. We explain the lower deactivation in the latter three cases with the significantly larger particle sizes in these studies, which are less susceptible to sintering.

Finally, the deactivation behaviour of reductively conditioned catalysts in a H_2-rich atmosphere is displayed in figure 5b. In this case the general behaviour differs strongly from that of the previous cases, showing is an initial increase in activity during the first 300 min rather than the normal strong initial decrease. Following that initial activation phase the activity is very stable, comparable to the trend observed for the calcined samples in H_2-rich atmosphere. The absolute amount of the initial activation (increase of the reaction rate from 17 min to 300 min) is between 53% and 109%. On the other hand, even after the initial activation phase the absolute activity of the reductively conditioned catalysts is still slightly lower than that of the calcined catalysts.

Also in these experiments the agreement between the different catalysts is not as good as for the calcined catalysts. Again catalyst Au/TiO_2(E) shows a worse performance than the other catalysts with the same loading, and equally to observations after redox-conditioning, it has the highest Au^{3+} amount of all samples. This points to an involvement of the Au^{3+} species in the lower activity of sample (E). A lower activity on Au^{3+} containing Au particles, i.e., not fully reduced particles, would explain also the initial activation phase. In that case the slight deactivation expected from comparison with the behaviour of the calcined catalysts could be overcompensated by an increase of the reaction rate due to slow reduction of the Au^{3+} species during reaction. Finally the high loading catalyst Au/TiO_2(D) is again less active than the other three low-loading catalysts, similar to the observations for the calcined samples.

We had previously tested the reductive conditioning also with a pure anatase supported catalyst, and in that case no such activation behaviour was observed [11]. Hence, the activation must be related to the presence of rutile in the Degussa P25 support material.

In the only earlier study on the deactivation of a reductively conditioned catalyst Lin *et al.* reported a slight deactivation upon reaction at 40 °C for a catalyst prepared *via* the incipient wetness method and subsequent reduction in H_2 for 1 h at 500 °C, in the presence of excess O_2 [15]. The deactivation was stronger when the O_2 excess was reduced. When comparing with our results it should be noted that their reduction temperature was 300 °C higher than the one used here and that the reaction was carried out in a H_2-free atmosphere. The absence of an activation phase for higher reduction temperatures agrees with our above interpretation that the initial activation of the low temperature (200 °C) reduced catalyst during the initial stages of the reaction in a H_2-rich atmosphere is due to continuing reduction of the catalyst, until this is completely reduced.

3.2.3. *Selectivity after calcination and reductive conditioning*

In figure 6 the selectivity of the catalysts in H_2-rich atmosphere after calcination and reductive conditioning is shown. The selectivity is defined here by the amount of O_2 consumed for CO oxidation, divided by the total amount of O_2 consumed, and calculated from the balance between CO_2 formation and O_2 consumption [20] (It should be noted that this is only correct as long as the H_2 level is not affected by any other reaction such as the water–gas shift (WGS) reaction ($CO + H_2O \leftrightarrow CO_2 + H_2$) or the methanation reaction ($CO + 3H_2 \leftrightarrow CH_4 + H_2O$), which appears justified based on previous measurements of the forward WGS reaction on a Au/TiO_2 catalyst under comparable conditions by Sakurai *et al.* [42]).

Similar to the activity during reaction in the H_2-rich atmosphere (figure 5a and b) also the selectivity changes little with time and exhibits rather constant values. After calcination the selectivity is in the range between 40% and 65%, after reductive conditioning it is significantly lower, between 25% and 45%. The stability of the signals is less than that for the CO oxidation rates, which reflects the problems in measuring small differences in relatively large O_2 partial pressures, and also the differences between different catalysts are larger than in the activities. These plots do not, however, show any effect

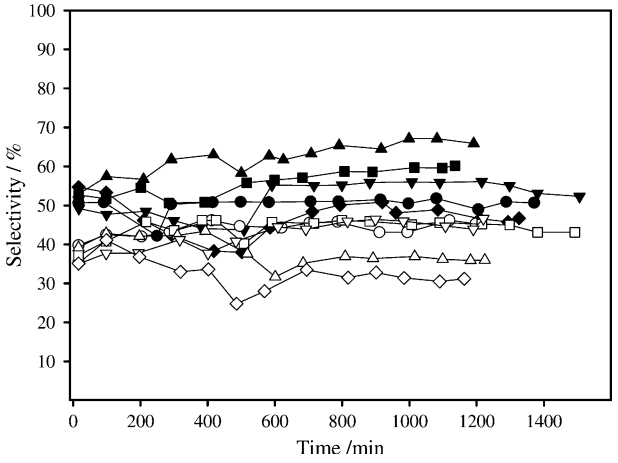

Figure 6. Selectivity of the calcined catalysts (filled symbols, measurements of figure 5a) and the reductively conditioned catalysts (empty symbols, measurements of figure 5b) in a H_2-rich atmosphere (1 kPa CO, 1 kPa O_2, 75 kPa H_2, blance N_2) . ○: Au/TiO_2(A), □: Au/TiO_2(B), △: Au/TiO_2(C), ∇: Au/TiO_2(D), ◇: Au/TiO_2(E). For more clarity not all data points are shown.

of the lower activity of catalyst (E) nor of the initial activation phase of the reductively conditioned catalysts. Therefore, whatever is responsive for these effects, does not affect the selectivity, or in another way, it equally affects the probability for CO oxidation and for H_2 oxidation. The most plausible explanation for the lower activity of the respective catalysts – catalyst (E) in for the redox and reductively conditioned catalysts and the reductively conditioned catalysts before their initial activation phase – is therefore a reduced activity for O_2 activation (O–O bond breaking). This may be related to the presence of Au^{3+} species, but definite proof for that is still missing.

The physical reason for the higher selectivity of the calcined catalysts is not yet clear. It may be related to the larger Au particle sizes in these samples (see table 1) or to the presence of Au^{3+} on the reductively conditioned catalyst (see table 2). The latter explanation, however, would contradict the above tentative assumption that a change in Au^{3+} content does affect the activity, but not the selectivity. So a satisfactory explanation is still awaited.

Previous studies on the selectivity for CO oxidation in a H_2-rich atmosphere and its stability with time are scarce. Choudhary *et al*. reported a selectivity of 72% at a reaction temperature of 80 °C ($CO:H_2:O_2:He = 1:50:2:25$, p_{tot} = 1000 mbar) [17]. This value is at the upper limit of our data for the calcined catalyst. In our previous study of selective CO oxidation on an anatase supported Au/TiO_2 catalyst (conditioning: calcination at 400 °C) we obtained a selectivity of ~45% for comparable reaction conditions; which is in the range of the present data for the calcined samples [12]. Hence the presence of rutile in the P25 support material does not influence the selectivity for CO oxidation in a H_2-rich atmosphere. Similar values were also reported by Schubert *et al*. for a catalyst pretreated by calcination at 400 °C (80 °C reaction temperature), who also observed little change in the selectivity with time [21].

4. Summary

In summary we have demonstrated that highly active Au/TiO_2 catalysts, with initial activities (TOF) $> 2\ s^{-1}$, can be prepared in a well-defined and reproducible way using a deposition–precipitation method reported earlier [11] and P25 as support material. Comparing five different catalysts prepared separately, four of them with the same Au loading of around 3 wt% and one with about 5 wt%, and each of the samples conditioned in three different ways we find very similar particle sizes and particle size distributions for the different catalysts, with mean particle sizes of ~3 nm for the calcined catalysts and of ~2 nm for the reductively and redox conditioned catalysts. The subsequent oxidation cycle in the redox conditioned catalysts does not lead to an additional Au particle growth compared to the reductively conditioned catalysts. For all catalysts we obtain fully reduced Au nanoparticles after calcination, while after reductive and redox conditioning small amounts of Au^{3+} species are resolved. The activity for CO oxidation and its deactivation with time depends mainly on the reaction atmosphere and on the conditioning procedure. The calcined catalysts show very good agreement between the different samples, with initial TOF numbers between 3 s^{-1} and 4 s^{-1}, which is similar to values reported for good catalysts in the literature, and a decay activity to about 10–35% of the initial activity over 1200 min. for reaction in H_2-free atmosphere, while in H_2-rich atmosphere the deactivation is much less pronounced. In both reaction atmospheres we find a lower activity for the higher loading sample.

For the two other conditioning procedures the agreement between different samples is not as good as for the calcined samples, with one sample showing a stronger deactivation than the other ones. For reaction of the redox conditioned samples in H_2-free atmosphere we find a similarly strong deactivation as for the calcined samples, resulting in activities of 10–35% of the initial value after 1000 min on stream. For reaction of the reductively conditioned catalysts in H_2-rich atmosphere we find an initial activation during the first 300 min on stream and no significant deactivation in the later stages. The activation process is tentatively attributed to the complete reduction of the Au^{3+} species on the catalyst during reaction. The activation process does not lead, however, to higher rates as observed for the calcined catalysts. The selectivity in for CO oxidation in H_2-rich atmosphere was found to be stable with time, independent of conditioning procedure, and significantly higher, by about almost 20%, for the calcined samples.

Acknowledgments

We gratefully acknowledge financial support by the Deutsche Forschungsgemeinschaft within the Priority Programme 1091 (Be 1201/9–3).

References

[1] M. Haruta, Catal. Surv. Jap. 1 (1997) 61.
[2] G.C. Bond and D.T. Thompson, Gold Bull. 33 (2000) 41.
[3] G.C. Bond, Catal. Rev. Sci. Eng. 41 (1999) 19.
[4] M. Haruta, CATECH 6 (2002) 102.
[5] F. Boccuzzi and A. Chiorino, J. Phys. Chem. B 104 (2000) 5414.
[6] G.R. Bamwenda, S. Tsubota, T. Nakamura and M. Haruta, Catal. Lett. 44 (1997) 83.
[7] Y. Iizuka, H. Fujiki, N. Yamauchi, T. Chijiiwa, S. Arai, S. Tsubota and M. Haruta, Catal. Today 36 (1997) 115.
[8] M. Haruta, S. Tsubota, T. Kobayashi, H. Kageyama, M.J. Genet and B. Delmon, J. Catal. 144 (1993) 175.
[9] F. Boccuzzi, A. Chiorini, M. Manzoli, P. Lu, T. Akita, S. Ichikawa and M. Haruta, J. Catal. 202 (2001) 256.

[10] J.-D. Grunwaldt and A. Baiker, J. Phys. Chem. B 103 (1999) 1002.
[11] B. Schumacher, V. Plzak, M. Kinne and R.J. Behm, Catal. Lett. 89 (2003) 109.
[12] B. Schumacher, Y. Denkwitz, V. Plzak, M. Kinne and R.J. Behm, J. Catal. 224 (2004) 449.
[13] A. Wolf and F. Schüth, Appl. Catal. 226 (2002) 1.
[14] M.J. Kahlich, H.A. Gasteiger and R.J. Behm, J. Catal. 182 (1999) 430.
[15] S.D. Lin, M.A. Bollinger and M.A. Vannice, Catal. Lett. 17 (1993) 245.
[16] M.A. Bollinger and M.A. Vannice, Appl. Catal. B 8 (1996) 417.
[17] T.V. Choudhary, C. Sivadinarayana, C.C. Chusuei, A.K. Darye, J.P. Fackler and D.W. Goodman, J. Catal. 207 (2002) 247.
[18] J.F. Moulder, W.F. Stickle, P.E. Sobol and K.D. Bomben, *Handbook of X-ray Photoelectron Spectroscopy* (Perkin Elmer Corp., Eden Prairie/USA, 1992).
[19] P.B. Weisz, Chem. Engin. Progr. Symp. Ser. 55 (1992) 29.
[20] M.J. Kahlich, H.A. Gasteiger and R.J. Behm, J. Catal. 171 (1997) 93.
[21] M.M. Schubert, V. Plzak, J. Garche and R.J. Behm, Catal. Lett. 76 (2001) 143.
[22] F. Boccuzzi, A. Chiorino and M. Manzoli, Surf. Sci. 454–456 (2000) 942.
[23] R. Zanella, S. Giorgio, C.-H. Shin, C.R. Henry and C. Louis, J. Catal. 222 (2004) 357.
[24] M. Daté, Y. Ichihashi, A. Chiorino, F. Boccuzzi and M. Haruta, Catal. Today 72 (2002) 89.
[25] N.J. Ossipoff and N.W. Cant, Top. Catal. 8 (1999) 161.
[26] S. Kielbassa, M. Kinne and R.J. Behm, Langmuir, in press.
[27] S. Schimpf, M. Lucas, C. Mohr, U. Rodemerck, A. Brueckner, J. Radnik, H. Hofmeister and P. Claus, Catal. Today 72 (2002) 63.
[28] M. Manzoli, A. Chiorino and F. Boccuzzi, Surf. Sci. 532–535 (2003) 377.
[29] H.-G. Boyen, G. Kästle, F. Weigl, B. Koslowski, C. Dietrich, P. Ziemann, J.P. Spatz, S. Riethmüller, C. Hartmann, M. Möller, G. Schmid, M.G. Garnier and P. Oelhafen, Science (2002)..
[30] J.M.C. Soares, P. Morrall, A. Crossley, P. Harris and M. Bowker, J. Catal. 219 (2003) 17.
[31] R. Holm and S. Storp, Appl. Phys. 9 (2003) 217.
[32] T. Dickinson, A.F. Povey and P.M.A. Sherwood, J. Chem. Soc. Faraday Trans. 71 (1974) 298.
[33] J.-C. Dupin, D. Gonbeau, P. Vinatier and A. Levasseur, Phys. Chem. Chem. Phys. 2 (2000) 1319.
[34] G. Martra, Appl. Catal. A 200 (2000) 275.
[35] E.D. Park and J.S. Lee, J. Catal. 186 (1999) 1.
[36] P. Konova, A. Naydenov, Cv. Venkov, D. Mehandjiev, D. Andreeva and T. Tabakova, J. Mol. Catal. A 213 (2004) 235.
[37] S. Arrii, F. Morfin, A.J. Renouprez and J.-L. Rousset, J. Am. Chem. Soc. 126 (2004) 1199.
[38] K. Mallick and M.S. Scurrell, Appl. Catal. A 253 (2003) 527.
[39] M. Okumura, S. Nakamura, S. Tsubota, T. Nakamura, M. Azuma and M. Haruta, Catal. Lett. 51 (1998) 53.
[40] S. Tsubota, T. Nakamura, K. Tanaka and M. Haruta, Catal. Lett. 56 (1998) 131.
[41] M. Valden, S. Pak, X. Lai and D.W. Goodman, Catal. Lett. 56 (1998) 7.
[42] H. Sakurai, A. Ueda, T. Kobayashi and M. Haruta, Chem. Commun. (1998) 271.